Functional imaging of hippocampal layers using VASO and BOLD on the Next Generation (NexGen) 7T Scanner

Authors
Suvi Häkkinen, [1*] Alexander Beckett, [1,2] Erica Walker, [1,2] Laurentius Huber, [3] David A. Feinberg[1,2]

Affiliations
[1]Helen Wills Neuroscience Institute, University of California, Berkeley, Berkeley, CA, United States
[2]Advanced MRI Technologies, Sebastopol, CA, United States
[3]Martinos Center, MGH, Harvard Medical School, Charlestown, United States

***Corresponding author**: Suvi Häkkinen (shakkinen@berkeley.edu)

Abstract

Spatial accuracy and venous biases are a central concern in mesoscale fMRI, with subcortical brain regions facing additional challenges due to lower sensitivity, high physiological noise, and complicated vasculature. Here, we optimized CBV VASO on the NexGen 7T scanner for layer-specific investigations of the hippocampus. The presence of venous biases in VASO and BOLD (from the same acquisition) was then compared by using an established autobiographical memory task. While the activation patterns converged at macroscale, layer-specific differences emerged in the hippocampal subiculum, consistent with venous bias in the inner layers of the subiculum which can be explained by the unique two-sided venous drainage. Further, both VASO and BOLD supported an anterior-posterior dissociation between retrieval stages and functional connectivity with neocortical networks. Thus, hippocampal fMRI allows mapping layer function with high accuracy, and can provide deeper insights into a number of neuropsychological phenomena and the early changes occurring in Alzheimer's disease.

Keywords: fMRI, VASO, 7 Tesla, hippocampus, cortical depth analysis

Introduction

A central pursuit in mesoscale fMRI is to model activation flow in the columns and depths of gray matter (Felleman and Van Essen, 1991). So far, most efforts have focused on neocortical circuits, yet incorporating subcortical areas and circuits would be highly relevant for neuroscientific and clinical applications. The changes in the early and presymptomatic stages of Alzheimer's Disease (AD), for example, are deeply rooted in the subcortex, where pathology initially targets specific small structures (e.g. locus coeruleus and hippocampal subfield CA1; Kerchner et al., 2012; Mather and Harley, 2016) and specific cortical laminae (Braak and Del Tredici, 2020), and spreads in patterns strongly linked with structural and functional connectivity (Lace et al., 2009; Franzmeier et al., 2020; De Flores et al., 2022; Grieco et al., 2023). As such, 7T MRI with its higher SNR can be used to study AD by evaluating changes in brain structure and function with higher resolution that allows better resolving small structures, accurate subfield segmentation of hippocampus, and detecting microcircuitry changes with layer fMRI. Imaging hippocampal activity is extremely challenging due to its location far from the receiver coils, high levels of physiological noise, and its intricate functional and structural organization.

Human hippocampus is a critical structure with a layered organization with gray matter in parts less than 1 mm thick, complex curved shape, and functional specialization along short and long axes (Vos De Wael et al., 2018; Dalton et al., 2019; Zheng et al., 2021; Angeli et al., 2025), with studies emerging also on laminar functional differentiation (Maass et al., 2014; Ahmadi et al., 2024; Pfaffenrot et al., 2025; Warrington et al., 2025). In addition to the requirement for sufficiently small voxel size and detection sensitivity, hippocampal layer-fMRI faces the challenge of intricate subfield- and layer-dependent vasculature: blood may drain to either inner or outer surface depending on hippocampal region and individual anatomy (Duvernoy et al., 2005). A bias which makes it difficult to reliably localize BOLD activity in neurovascular coupled activation is that blood oxygenation changes are also in the cortical draining veins, creating a confound in differentiating changes in layer activity (Duvernoy et al., 1981; Olman et al., 2007). Therefore, contrast mechanisms that are inherently less sensitive to the large draining veins (Oshio and Feinberg, 1991; Lu et al., 2003; Feinberg et al., 2008) would be very attractive for hippocampal layer-fMRI, but remain challenging in practice.

VAscular Space Occupancy (VASO) contrast is able to localize neuronal activity with high spatial specificity based on changes in cerebral blood volume (CBV), primarily the dilation of arterioles, capillaries, and intracortical arteries. The VASO contrast and its lesser sensitivity to large draining veins has been validated using animal models and invasive imaging techniques (Huber et al., 2021), and commonly used in neocortical layer-fMRI. The gain in specificity comes, however, at the cost of lower signal-to-noise ratio (SNR) and contrast-to-noise (CNR) of roughly half compared to BOLD at 7T due to larger venous deoxyhemoglobin dependent changes compared to microvascular blood volume changes (Huber et al., 2014, 2015; Beckett et al., 2020). Thus, reaching sufficient detection power with VASO in submillimeter hippocampal imaging may be challenging. Further, the pulse sequence and the lower statistical power of the contrast often necessitate the use of relatively long TRs and block designs, limiting the types of neuroscientific inquiries. Recent research however shows promise in applying VASO in high-noise subcortical (Rane et al., 2016; Burak et al., 2022; Ahmadi et al., 2025) and auditory (Faes et al., 2023) regions as well as in rapid short TR experiments (Dresbach et al., 2023). In this

work, we will apply VASO to study hippocampal layers at the Next Generation (NexGen) 7T scanner (Feinberg et al., 2023). The NexGen 7T incorporates many high-performance components specifically adapted for mesoscale imaging at 7T, including high-channel array coils and a head-only asymmetric gradient coil ("Impulse") with ten times higher performance than the body gradient coil available on standard 7T systems. This advanced hardware on NexGen 7T allows for better optimization for high-resolution imaging in hippocampus, through improved acceleration performance and SNR from the high-channel array, and reduced EPI readout time using the shorter echo spacing allowed by the head gradient coil. Thus, the scanner allows the opportunity for further VASO sequence optimization.

The recall of autobiographical memories rich in detail and context reliably activates hippocampus in fMRI (Addis et al., 2007; Leelaarporn et al., 2024; Pfaffenrot et al., 2025). In the present study, we applied an established autobiographical memory paradigm to assist in the interpretation and validation of VASO contrast results. We assess activation based on VASO and BOLD contrasts, from the same acquisition, in terms of 1) sensitivity to detecting hippocampal activation during an autobiographical memory task, 2) ability to detect venous bias through comparison of VASO and BOLD from the same acquisition, and 3) the feasibility of detecting temporal dynamics during memory retrieval, requiring sensitivity to shorter blocks. In addition, we assess their ability to resolve functional connectivity between hippocampal and neocortical areas. Together these results will inform on the sensitivity and specificity of VASO and BOLD to hippocampal activity, as well as on their capability in serving different experimental setups.

Results

VASO and BOLD activation to autobiographical memory task

To assess the capability of VASO and BOLD in detecting hippocampal activation, we measured activation during an established autobiographical memory task paradigm. Contrasting autobiographical memory and mental arithmetic conditions revealed that, at macroscale, VASO and BOLD patterns converged in the cortex as well as hippocampus (**Figure 1**; for neocortical group mean patterns see **Figure 5A**). As expected, BOLD had higher detection sensitivity as measured by individual level z-scores.

For finer-grained analysis, hippocampus was segmented by subfield and layer (**Figure 2A**–**B**). Memory-related activation patterns (AM > MA) for VASO and BOLD were similar with pronounced activation in the anterior hippocampus (**C**; see also individual maps in **Supplementary Figure S2**). Activation (beta values) reached group-level significance for BOLD (one-tailed cluster-based inference, FWE-corrected at $p < 0.05$ using a primary voxel-level threshold of $Z > 2.1$). VASO activation did not survive cluster correction except with stronger NORDIC denoising (factor error level of 1.5), which is likely explained by the lower statistical sensitivity of VASO and the small sample size. In an initial look at layer dynamics, both VASO and BOLD suggested stronger activation in inner compared outer layers (**D**) though the statistic distributions also showed differences, particularly with relative emphasis of subicular inner layer activation in BOLD discussed below. Intriguingly, the differences in layer activation reached group-level significance with VASO and not BOLD, and with VASO at NORDIC factor noise level 1 but not 1.5. These observations may reflect the higher depth localization accuracy

of VASO compared to BOLD and caveats of NORDIC denoising. Given the limited sample size, the current conclusion is that both VASO and BOLD detect hippocampal activation.

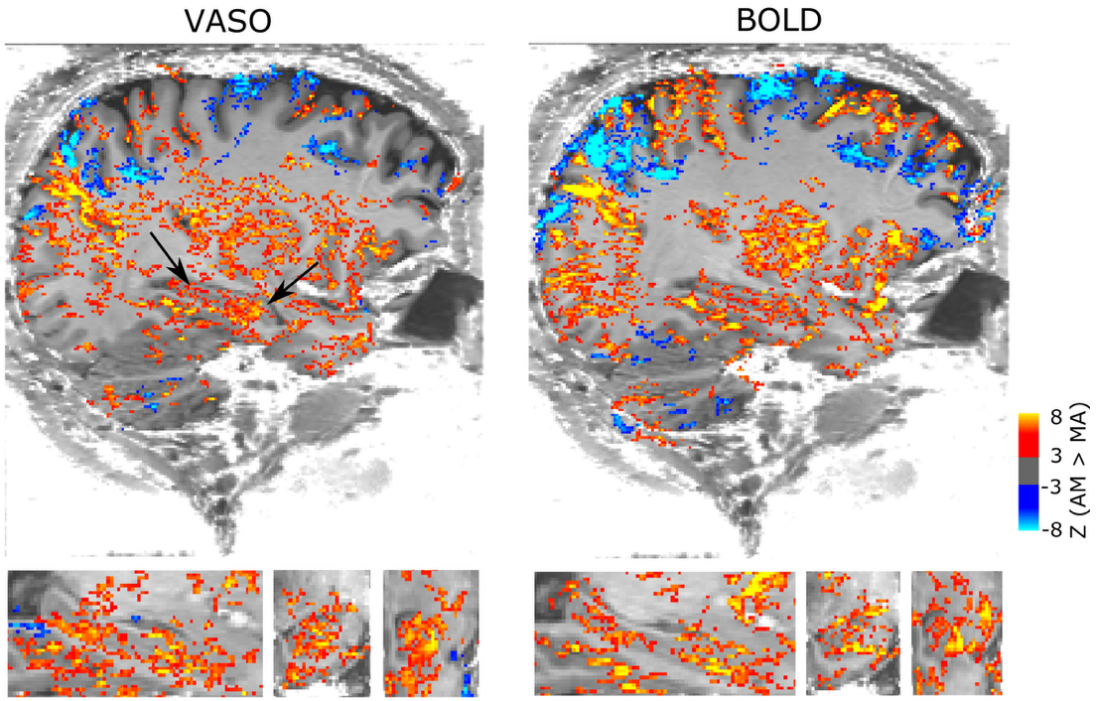

Figure 1. Consistent macroscale activation for VASO and BOLD during memory task (AM > MA). This analysis was based on two sessions (70 minutes) of data. For this macroscale visualization only, VASO and BOLD were denoised with NORDIC factor error levels of 1.5 and 1.0, respectively, to highlight the noisier VASO pattern. Both were thresholded at Z > 3 and clusters of 100 voxels (AFNI *3dClusterize*).

The specificity of VASO and BOLD in detecting layer activation was then assessed based on z-scores at different depths of gray matter, revealing subtle differences. In line with the known venous drainage pattern in the subiculum towards the inner surface (**Figure 3A**; Duvernoy et al., 2005), the activation profile shapes revealed stronger BOLD activation during the memory task in the inner layers (**B**). The VASO–BOLD difference was seen quite systematically also at individual participant level, with an absent or reversed effect in VASO. These visual observations on subicular activation were confirmed by group-level ROI PTA analysis (**C**), in which a significant Contrast × Layer interaction confirmed different profile shapes between VASO and BOLD, and the evidence plot relatively stronger BOLD activation in the inner layers. The ROI PTA analysis indicated systematic differences between the VASO and BOLD layer profiles also in the three other subfields.

The relationships of VASO and BOLD in subiculum and CA1 were quite robust to preprocessing choices related to physiological noise regressors (**Supplementary Figure S3**) and NORDIC denoising (**Supplementary Figure S4**). Specifically, NORDIC denoising greatly facilitated the detection of VASO patterns in our hippocampal VASO dataset by increasing z-scores without

fundamentally changing layer profile shape. Some effect sizes (namely beta estimates in the inner layers of CA1; **Supplementary Figure S4**) were however reduced, which may result from signal components not being separable from the thermal noise in high noise datasets (Kay, 2022; Olesen et al., 2023; Faes et al., 2024).

To test the reliability of data and VASO–BOLD distinctions in 35 min acquisitions, we collected two sessions on one representative participant. The key results of VASO–BOLD difference in the inner layers of subiculum and similarity in CA1 are visible in individual sessions as well as in a combined analysis (**Supplementary Figure S5**).

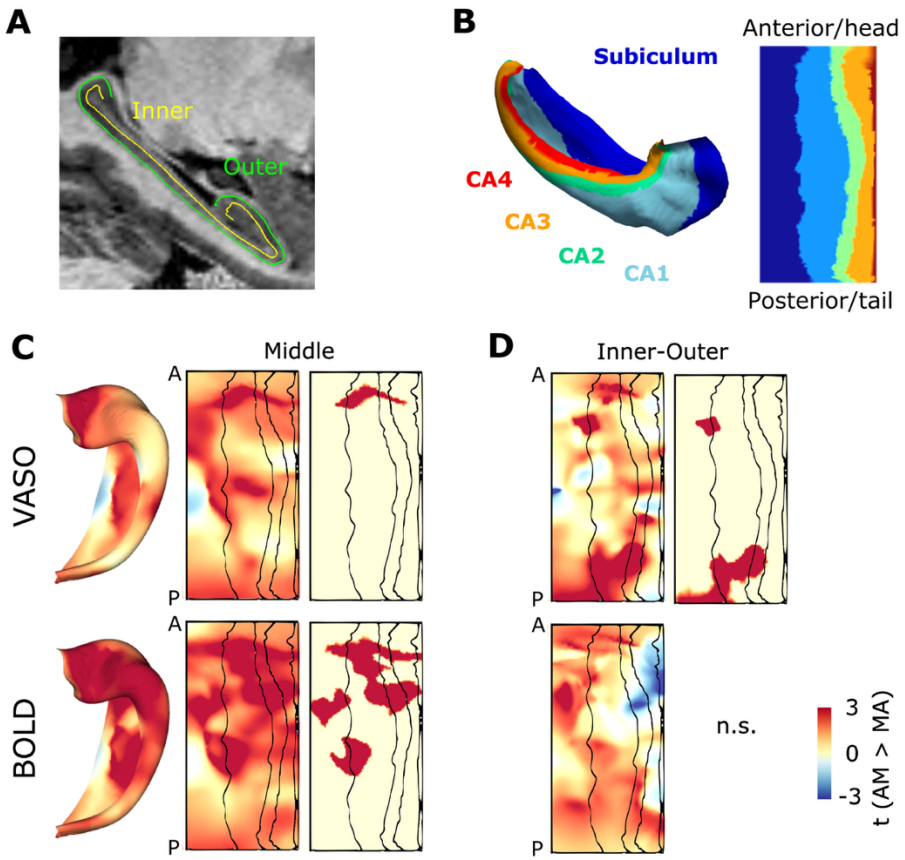

Figure 2. Hippocampal memory task activation (AM > MA) based on VASO and BOLD from the same acquisition. (**A**) Hippocampal inner and outer layers overlaid on sagittal MP2RAGE. (**B**) Hippocampal subfield segmentation on folded and unfolded hippocampal surfaces. (**C**) Group activation patterns visualized on unfolded surfaces (5 mm surface smoothing). T-statistic distributions suggested similar anterior emphasis in VASO and BOLD (left panel). BOLD showed significant clusters across the anterior subfields (right; N = 6; one-tailed $p < 0.05$, cluster-corrected at $Z > 2.1$). VASO activation survived cluster correction with stronger NORDIC denoising (factor noise level 1.5). (**D**) Comparison of task activation in the inner and outer layers suggested predominantly stronger activation in inner layers for both contrasts. Layer activation differences survived cluster correction only for VASO.

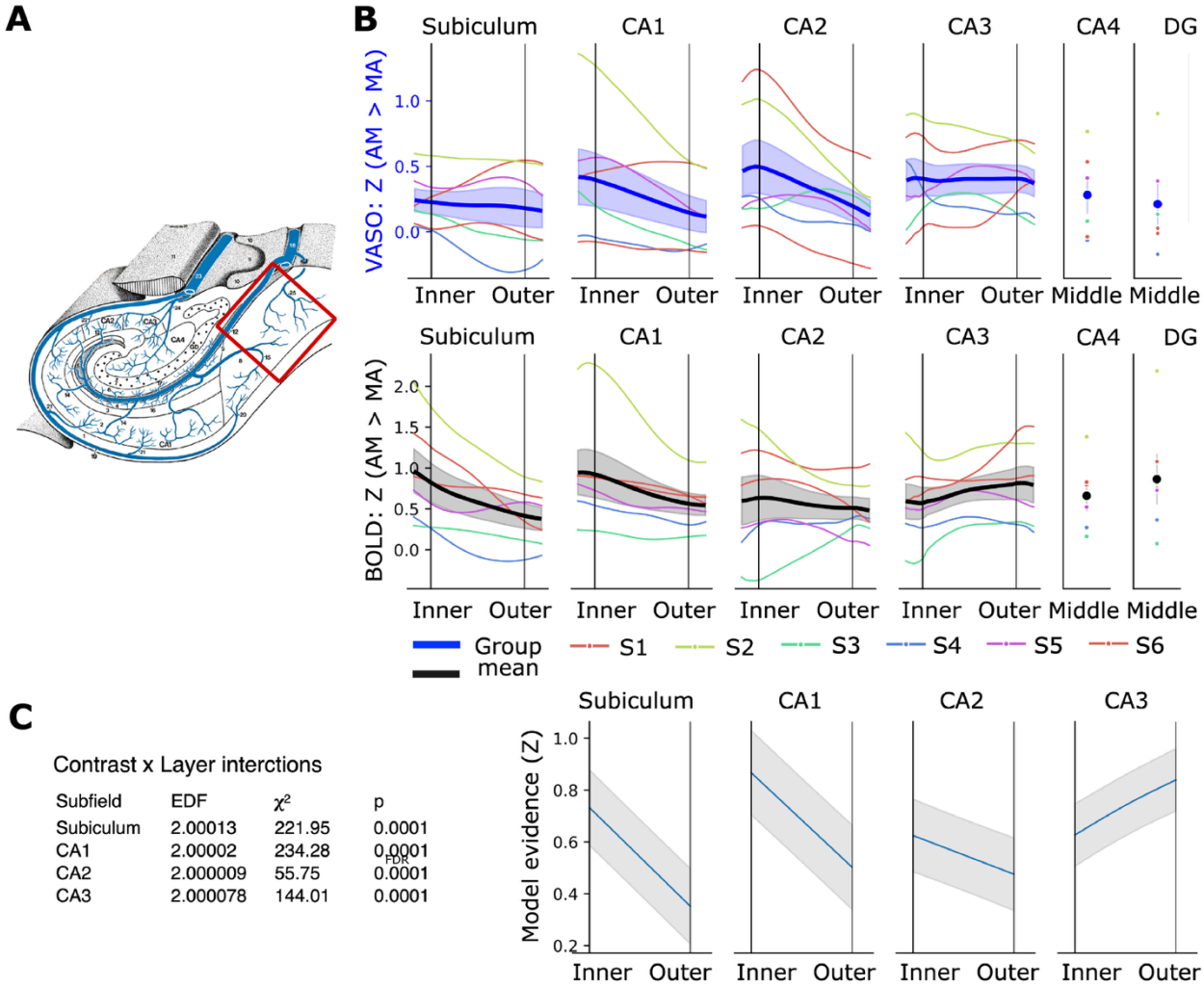

Figure 3. Layer-specific memory task activation (AM > MA) based on VASO and BOLD. (**A**) Schematic of hippocampal venous drainage patterns (modified from Duvernoy et al., 2005), with the inner layers' venous bias in subiculum highlighted. (**B**) ROI analysis of memory task layer activation per hippocampal subfield. Note the stronger activation in the inner layers of subiculum in the BOLD but not VASO results, consistent with a venous bias. In CA1, stronger inner layer activation is suggested by both contrast mechanisms. (**C**) ROI-based PTA analysis comparing the shapes of VASO and BOLD layer profiles using multilevel smoothing splines indicated differences in the inner layers of the subiculum and systematic differences also in other subfields. In (**B**–**C**), shaded area corresponds to standard error.

Finally, we explored activation differences between the construction and subsequent elaboration stage of autobiographical memory recall, known to have partially distinct neuronal correlates. The methodological challenge with this comparison is the speed of these dynamics, as reconstruction duration is similar to our TR of 3.2 s ("AM response time" in **Supplementary Table S1**). Both VASO and BOLD activation patterns showed trends of an anterior-posterior distinction (**Figure 4A;** individual maps in **Supplementary Figure S6**), with the elaboration

stage associated with relatively stronger activation in the posterior hippocampus and its inner layers (**B**). These trends were however not significant at corrected thresholds. Layer profiles (averaged per subfield) also did not reveal consistent differences across participants, probably due to heterogeneity along the long axis.

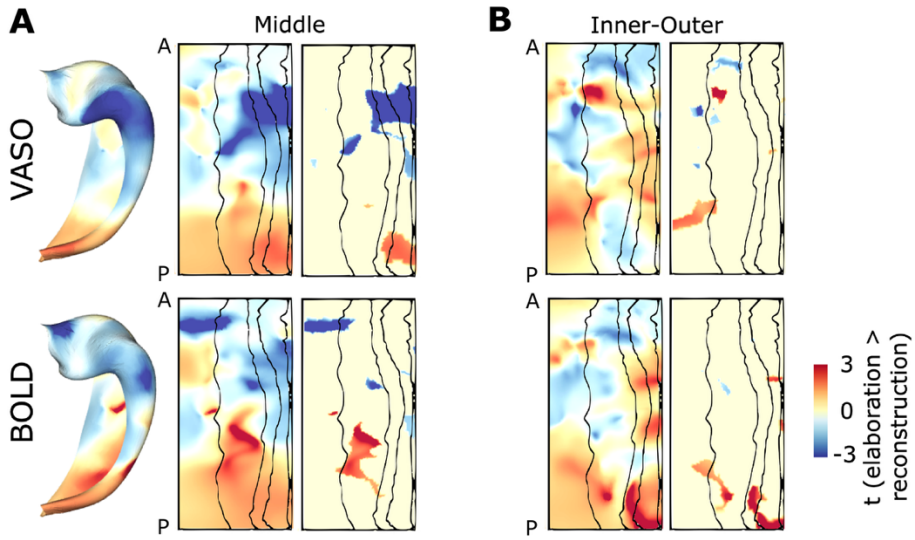

Figure 4. Exploratory analysis of memory retrieval stage dependent activation (elaboration > construction) based on VASO and BOLD from the same acquisition. (**A**) Group average activation patterns visualized on unfolded surfaces (5 mm surface smoothing), trending towards an anterior-posterior distinction. (**B**) Comparison of inner and outer layer activation, with both contrasts suggesting that elaboration is associated with relatively stronger activation particularly in the inner layers of posterior hippocampus. In (**A**–**B**), the left panel shows t-statistic distribution and the right panel t-values thresholded to uncorrected one-tailed $p < 0.05$.

Hippocampal neocortical connectivity

Functional connectivity patterns were expected to show some resemblance to the task-evoked activation patterns (**Figure 5A**). The neocortical activation patterns were spatially fine-grained. At group level, activation was stronger during AM than MA task in prefrontal, visual and motor cortices (red). MA, in turn, showed stronger VASO and BOLD activation in for example inferior parietal regions (blue).

Comparison of the relative differences in the connectivity of anterior and posterior hippocampus (**Figure 5B**) showed that posterior subiculum more strongly connects to areas also activated for the AM than MA task. The spatial pattern was clearer in BOLD than VASO, likely explained by the lower SNR in VASO.

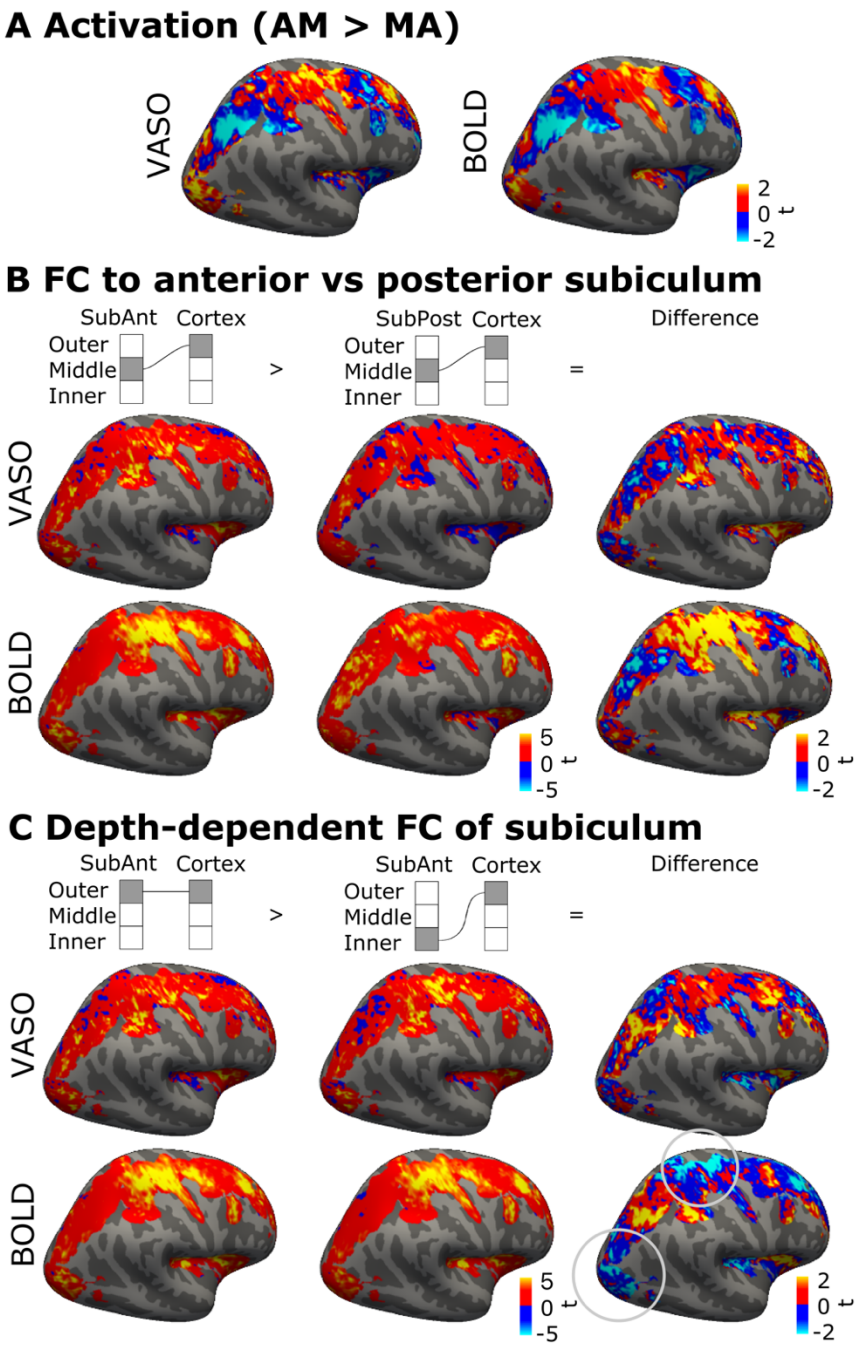

Figure 5. Neocortical activation and hippocampal functional connectivity patterns based on VASO and BOLD, in the group of six subjects. (**A**) Converging activation patterns (AM > MA) indicated functionally distinct areas. (**B**) Functional connectivity (FC) patterns associated with anterior and posterior subiculum, a major output region of the hippocampus, showed relative anterior–posterior differences. (**C**) Connectivity seeded by inner and outer depths of anterior subiculum, a region with a known outer-to-inner venous bias. Depth-dependent differences based on VASO and BOLD show differences (circled). In (**A**–**C**), statistics are shown only for the right hemisphere vertices imaged in all six participants.

In the analysis of depth-dependent connectivity, both VASO and BOLD showed for example that connectivity to most neocortical areas more activated by math (MA > AM) was stronger from the outer than inner layers of the subiculum (**Figure 5C**; red). Connectivity patterns were also visually quite similar, showing for example a clearly different depth-dependent connectivity pattern of CA3 compared to the other subfields (**Supplementary Figure S7**). The depth-dependent connectivity patterns obtained with VASO and BOLD however also showed differences. Depth-dependent patterns of the subiculum, with a known strong venous bias, showed pronounced VASO–BOLD differences. Notably, these differences occurred in areas showing stronger activation during memory task (blue in **A**), and all in the direction of BOLD suggesting stronger subiculum inner than outer layer connectivity. Thus, the difference might be driven by the venous signal reflected in BOLD based connectivity, misplacing signal fluctuations from outer to inner layers of subiculum leading to over-estimation of inner-layer activity.

Discussion

This study demonstrates that CBV VASO is an effective tool for investigating hippocampal circuitry, in the context of an established autobiographical memory task. Concurrently acquired VASO and BOLD differed in the suggested layer-resolution localization of activation and connectivity, consistent with a dominant venous signal in BOLD obscuring depth-dependent distinctions in activity. While several task activation effects were observed quite similarly using both contrasts, others were obscured by the venous biases in BOLD, producing clear mislocation (subiculum) and possible artifactual amplification (CA1) of task effects of interest. VASO is therefore a strong alternative for studies on circuit mechanisms where cortical depth-specificity is critical.

VASO and BOLD differences in activation are consistent with venous bias in hippocampus

VASO and BOLD results converged well at the macroanatomical level, indicating activation in the hippocampus during autobiographical retrieval (AM > MA; **Figure 1**), stronger activation (AM > MA) in the anterior than posterior hippocampus **(Figure 2C**), and during elaboration compared to construction stage of the memory task (**Figure 4A**). As expected, however, VASO and BOLD results differed at layer resolution.

The dual contrast fMRI approach used here with VASO and BOLD extracted from the same acquisition allowed us to identify which BOLD layer profiles can be interpreted with respect to neuronal laminar circuitry and which profiles need to be considered as vascular biases. In particular, we planned to use subiculum as a test case, as previous literature is clear that the blood in subiculum is drained through veins along the inner surface (Duvernoy et al., 2005), with respective expected artifactual fMRI signal misplacement (Haast et al., 2024; Pfaffenrot et al., 2025). The activation results in the subiculum clearly show a VASO–BOLD mismatch with more activation in the inner layers using BOLD than VASO, implying less bias in VASO (**Figure 3B–C**). Thus, a BOLD based analysis might lead to the interpretation that input-receiving outer layers of the subiculum are less active, and the inner output layers more active, than they truly are.

Contrasting with the clearcut difference between VASO and BOLD results in the subiculum, results were quite different in CA1, which also has a prominent (outer to inner) vascular bias. In CA1, both VASO and BOLD contrasts indicated stronger activation in inner than outer layers (AM > MA; **Figure 3B**), suggesting that there is a true task-related activation difference between depths of CA1. This finding aligns with the previous layer-BOLD study (Pfaffenrot et al., 2025), which compared responses to the autobiographical task and hypercapnic challenge, and found them both associated with greater CA1 inner layer activation but with distinct laminar response shapes. They concluded that while venous bias is not the sole driver of this inner layer CA1 response, results in the area should be interpreted with caution. The observed depth-specific pattern is also in line with greater input to CA1 from the trisynaptic pathway (DG → CA3 → CA1), compared to the perforant path (entorhinal cortex → CA1), which terminate in inner and outer layers of CA1, respectively (Amaral and Witter, 1989). Specifically the trisynaptic pathway has been widely implicated in pattern completion such as retrieval of specific episodic memories (Rolls, 2013). In cases such as CA1 during autobiographical memory recall where neuronal and vascular responses are very similar, VASO contrast may provide a well-principled way to disentangle their relative contributions.

Also CA2 and CA3 showed systematic differences between VASO and BOLD layer profiles in our layer profile shape analysis, with BOLD showing pronounced activation in the inner layers of CA2 and outer layers of CA3 (**Figure 3C**). Our result is consistent a small outward bias in CA3 reported in Pfaffenrot et al. (2025). These subfields are however commonly assumed to have a drainage both via inner and outer layers, and any population level biases should be confirmed in larger sample.

Beyond the subfield-specific differences, VASO and BOLD based results largely agreed on the specialization along the hippocampal long axis during memory retrieval (**Figure 4A**). The comparison of elaboration and construction stages of retrieval suggested further nuance: activation during elaboration was relatively stronger in the posterior than anterior hippocampus, and in the posterior hippocampus stronger in inner than outer layers (**B**). The posterior hippocampal emphasis to elaboration is consistent with previous studies contrasting these task stages (Audrain and McAndrews, 2022; Pfaffenrot et al., 2025) as well as with the theory that posterior hippocampus supports the retrieval of fine-grained details and anterior hippocampus coarser, gist-like memory features (Poppenk et al., 2013; Brunec et al., 2018; Audrain and McAndrews, 2022). The relative difference between the inner and outer layers of several posterior subfields is also in line with findings of the previous layer-BOLD study (Fig. S10K in Pfaffenrot et al., 2025). A possible circuitry level explanation might be continuous engagement of hippocampal pattern completion as more details are matched to the episodic event during elaboration: e.g., input from dentate gyrus to the inner layers of CA3 for pattern completion and from CA3 to the inner layers of CA1.

Neocortical activity and hippocampal connectivity

Hippocampus and neocortex are known to function in concert during memory retrieval. As our FOV captured some of the relevant neocortical areas, we were able to assess their interplay with the hippocampus. Based on visual comparison to known large-scale neocortical network patterns, autobiographical memory was associated with stronger activation in areas likely

overlapping with putative default mode or parietal memory networks (**Figure 5A**, red), strongly associated with autobiographical memory (DiNicola et al., 2020; Kwon et al., 2025), as well as in visual and motor cortices, which may reflect sensory reactivation (Hofstetter et al., 2012; Gilmore et al., 2021). The mental arithmetic task, in turn, showed stronger VASO and BOLD activation (blue) in frontoparietal network areas such as intraparietal sulcus (Dehaene et al., 2004).

The anterior emphasis in hippocampus for autobiographical memory retrieval (**Figure 2C**) is consistent with previous literature suggesting stronger anterior than posterior hippocampal connectivity to the default mode network (Vos De Wael et al., 2018; Tang et al., 2020; Zheng et al., 2021; Borne et al., 2023; Angeli et al., 2025). Posterior hippocampus, in turn, has been reported to have relatively stronger connectivity to parietal memory, visual and sensorimotor networks, though neocortical connectivity may also vary by hippocampal subfield. In this context, the finding that elaboration compared to construction was associated with stronger activation in the posterior hippocampus (**Figure 4A**) might relate to pronounced involvement of the parietal memory network, sensitive to familiarity and goal-oriented cognition. Further study of these hippocampal neocortical connections might help better characterize the memory-related networks.

To summarize, neocortical (macroscale) task activation based on VASO and BOLD converged (AM > MA; **Figures 1** and **2C**). Spatially similar neocortical patterns also emerged in analyses of hippocampal functional connectivity (**Figure 5**, **Supplementary Figure S7**). This sensitivity to different aspects of functional organization suggests that both contrasts can be used for mesoscale functional connectivity mapping. However, depth profiles of functional connectivity based on VASO and BOLD differed in the subiculum such that BOLD showed pronounced neocortical connectivity associated with the inner layers. Given that this difference is in the direction of potential BOLD signal displacement in the subiculum, it serves as a cautionary example on venous confounds in BOLD also in functional connectivity.

Impact of NexGen 7T scanner on mesoscale functional imaging

These methodological advances have exciting implications for noninvasive, in-vivo mapping of the microcircuits to and from the hippocampus in humans. Optimization of VASO imaging in the hippocampus required us to leverage the advantages of the high signal at ultra-high field and the unique hardware of the NexGen 7T scanner (Feinberg et al., 2023) to achieve high-resolution CBV-weighted imaging with sufficiently short TR to resolve the different subphases of autobiographical memory retrieval, and obtain sufficient SNR to overcome the reduced sensitivity of VASO when compared to BOLD. On standard 7T scanners, one or more of these parameters would need to be compromised for VASO imaging in this subcortical brain region. This novel hardware is being further optimized for mesoscale imaging and will become more available at other research centers. Outstanding challenges include expanding spatial coverage without sacrificing resolution or sensitivity, which would allow for functional connectivity analyses to infer information flow between close (e.g. entorhinal cortex, Koster et al., 2018; Zhang et al., 2023, or parahippocampus, Warrington et al., 2025) and distant neocortical regions involved in primary sensory and executive control networks.

Impact of vein-free layer-fMRI in the hippocampus in future applications

Vein-free laminar imaging of the hippocampus opens the door to investigating computational mechanisms behind any number of neuropsychological phenomena:

- Imaging layers of the hippocampus are critical for investigating neural correlates of episodic memory to understand how it orthogonalizes representations that minimize interference between experiences and also integrating information across episodes (Koster et al., 2018).
- While it is known that the hippocampus plays a crucial role in spatial navigation, the underlying circuit-level mechanisms are poorly understood (Ahmadi et al., 2024).
- Specific subtypes of epilepsy, such as Type III of focal cortical dysplasia (FCD) can be caused by cortical dyslamination associated with hippocampal sclerosis (Aitken et al., 2025).
- The layers and subfields of the hippocampus are differentially affected in dementia, particularly in Alzheimer's disease. Specifically CA1 region and entorhinal cortex layer II are critical early sites of damage and are linked to memory impairments (Gómez-Isla et al., 1996; Kerchner et al., 2012). Imaging the layered structure of the hippocampus can be a useful research tool to capture the development and propagation of this pathology in the living human brain.
- Mood and stress disorders show involvement of specific subfields and layers such as a retraction of CA3 dendrites, decreased neurogenesis and structural connectivity of dentate gyrus, and decreased BOLD activation in both these subfields (Leal and Yassa, 2018; Rutland et al., 2019).
- Post-mortem studies on schizophrenia consistently report alterations in the neuronal morphology and synaptic density in the hippocampus (Harrison, 2004). Emerging theories postulate layer-specific mechanisms, such as hallucinations explained by dysfunction in integrating predictions with sensory evidence (Haarsma and Kok, 2025).

In general, the vascular organization of hippocampus and other subcortical regions is less charted, but drainage patterns are less straightforward compared to the neocortex and there is variability between participants (Duvernoy et al., 2005; Haast et al., 2024). The venous confound may introduce noise and mislead conclusions on the directionality of information flow based on BOLD data (especially in areas where the direction of the bias is unknown or varies between participants), whereas VASO may provide an additional insight to neural activity. The ability to do vein-free imaging of the hippocampus can also be used to validate when BOLD localization of neural activity can be judged to be accurate (e.g., memory related activation in the inner layers of CA1, despite a likely bias in the same direction).

Looking beyond the hippocampus, the tools developed here provide a starting point for mapping layer-specific connections within lower brain areas of cortex and between neo-cortex and sub-cortex, in the context of cognitive neuroscience, clinical neuroscience, and neurology. Until now, more than 95% of all >300 published human layer-fMRI studies could solely focus on brain areas in the upper half of the brain (source: layerfmri.com/papers), limiting the potential to capture neural information flow across laminar microcircuits throughout the entire human brain. The methodology developed here helps the field overcome these limitations and finally address questions of many influential theories of brain function that posit laminar signals with origins

and destinations in distinct cortical layers and lower brain areas. Several exemplary theories such as Predictive Coding, Thalamocortical Loop Models, Limbic–Cortical Integration Models for Emotion and Decision-Making may now be directly tested in humans. We expect that the ever-advancing tools and improvements of high-resolution fMRI will ultimately transform our understanding of cognition in the awake, behaving human brain.

CBV based fMRI has been shown to provide high specificity in imaging neocortical and hippocampal layer activity, useful for identifying neurocircuitry changes in neurological disorders in humans. The presented techniques will enable non-invasive imaging of neuronal circuits in the human brain and studies of connectivity and microcircuitry changes in AD and related dementias.

Materials and Methods

Subjects

Six participants (5 female; age 23–44 years) were scanned for the main analysis, and two additional in vivo scan sessions were used to identify the capabilities and challenges of hippocampal layer-fMRI as well as to implement and validate the imaging protocol. The study protocol was approved by the office for protection of human subjects, UC Berkeley IRB, and each participant gave written informed consent before MRI data acquisition.

Data acquisition

Data were collected on the NexGen 7T scanner equipped with the high performance Impulse head-only gradient coil "Impulse gradient" with maximum amplitude and slew rate (Gmax 200mT/m, SR 900 T/m/s) and a 64-channel receive array coil (Feinberg et al., 2023). CBV weighted functional data were collected using a VASO sequence (Huber et al., 2014) with a skipped-CAIPI 3D EPI readout. On the NexGen 7T scanner, the shorter echo spacings achievable using the Impulse gradient reduced signal dropout in the temporal regions, and importantly allowed readout of the 3D image slab within a single inversion recovery (IR) cycle of blood labeling. Therefore a segmented approach across multiple IR cycles was not required, which reduced the phase artifacts arising from such a segmented acquisition (**Supplementary Figure S1**). The scan parameters were: Matrix Size 206×206×30, field of view (FOV) 175×163, slice thickness 0.84 mm, TE 13.6 ms, In-plane segmentation 3, GRAPPA $1x3_{z1}$, Bandwidth 1516 Hz, Echo Spacing 0.72 ms, TI1/TI2 939 ms/2097 ms, TR_{vol} 1.158 s, effective TR (nulled/not-nulled) 3.2 s. The FOV was positioned sagittally, covering the right hippocampus and frontoparietal cortex expected to also be sensitive to the task paradigm. For anatomical reference, a whole brain MP2RAGE scan was also collected (voxel size 0.75 mm isotropic, matrix size 300x300x208, TE 2.82 ms, TR 6000 ms, Partial Fourier 7/8, GRAPPA 3, TI1/TI2 800 ms/2750 ms).

Autobiographical memory task experiment

The task paradigm was adapted from previous studies on fine-grained hippocampal activation, which have demonstrated stronger activation across hippocampal subfields during *autobiographical memory* (AM) compared to *mental arithmetic* (MA) task (McCormick et al.,

2015; Leelaarporn et al., 2024; Pfaffenrot et al., 2025). In the AM task, participants were presented with a cue-word (e.g., coffee) and were instructed to recall an event from their personal past that took place less than three years ago and lasted less than a day. The participants were told to press a button when they had selected a memory and then silently think about the event in detail until the word disappears, as if experiencing it again. Unique cue-words were taken from the Clark and Pavio extended norms (Clark and Paivio, 2004) based on high Thorndike-Lorge frequency, imageability and concreteness, as originally in (Addis et al., 2007). In MA, participants were presented with a simple mathematical problem (e.g., 15 + 12; additions, subtractions, multiplications, divisions) which they were to solve, then press a button, and start iteratively adding 3 to the result until the instruction disappears. AM and MA tasks were presented in alternating blocks separated by short fixation blocks. Data collection was TR-locked to the beginning of each task or fixation block, and task blocks had duration of 6 TR and rest blocks one TR, leading to 19.3 s task blocks separated by 3.2 s fixation blocks. Functional data was collected in three runs of 11.6 min (total 35 min). To assess the reliability of functional responses, one participant was measured twice on different days (total 70 min).

Participants briefly practiced the tasks right before the scan. Task compliance during scanning was measured by recording response button presses and verbally confirmed after the scan. Five participants indicated their task performance consistently throughout data acquisition (>97% and 88% of trials in the AM and MA task, respectively; **Supplementary Table S1**), but button presses were by mistake not recorded for one participant. Data from all six participants was included in main analyses comparing AM and MA blocks, but the data from the participant without recorded motor responses was excluded from the task stage comparison.

Hippocampal subfield segmentation and layer extraction

The MP2RAGE was used to estimate hippocampal inner and outer surfaces and segmentation of subfields subiculum, cornu ammonis (CA) 1–4, and dentate gyrus (DG) using HippUnfold (version 1.4.1; DeKraker et al., 2022). The surfaces (with an approximate vertex spacing of 0.5 mm) were then transformed to VASO space to avoid resolution loss due to data interpolation: Registration of VASO and MP2RAGE was initialized by cortical rigid boundary-based registration (Greve and Fischl, 2009) and fine-tuned in hippocampal regions with ANTs' symmetric normalization (SyN) algorithm (version 2.5.0; Avants et al., 2008). The affine and nonlinear transforms were applied to inner and outer hippocampal surfaces to bring them to native functional space using Connectome Workbench (wb_command version 1.5.0, Marcus et al., 2011). Finally, 20 equi-volume surfaces between inner and outer surface and 5 surfaces extending outside these limits were generated (*wb_command -surface-cortex-layer*).

Neocortical layer extraction

Brain surfaces were reconstructed from high spatial resolution (0.75 mm isotropic) MP2RAGE scans using the submillimeter recon-all pipeline from FreeSurfer (Dale et al., 1999; Zaretskaya et al., 2018). Analogous to hippocampal surfaces, the white and pial surfaces were warped to VASO space using ANTS and used to generate 25 equivolume surfaces representing different cortical depths, with inner and outer depth represented by the third surface inside white and pial surfaces.

Functional activation analysis

Nulled and not-nulled series were motion-corrected to mean volume of the first run (AFNI 3dVolreg). Noise reduction with distribution corrected PCA (NORDIC PCA; version 4/22/2021; Moeller et al., 2021; Vizioli et al., 2021) was applied to nulled and not-nulled images separately, on magnitude only (Knudsen et al., 2025). VASO contrast data was generated using dynamic division (Huber et al., 2014), which involves temporal upsampling to better align the series of images with and without blood nulling, and was also applied to BOLD data. This provided VASO and BOLD time-series data acquired in the same acquisition, which we then analyzed separately using the same pipeline. Because BOLD and VASO signal changes are opposite in sign, the VASO signal was inverted for easier comparison.

Initial 2–5 upsampled volumes were disregarded based on automatic estimation (*NonSteadyStateDetector* implemented in Nipype, Gorgolewski et al., 2011). Activation was estimated in native voxel space using general linear models (GLM) as implemented in Nilearn (Abraham et al., 2014). Analyses used two designs. The first design matrix had two regressors of interest (AM, MA), and a contrast was defined to contrast the two tasks. The second, three task regressor design, further split AM condition into separate construction and elaboration stages based on the button press during the trial, and a linear contrast compared these two memory task stages. For the second design, only trials with button press were modeled, and the one participant (S3) without recorded button presses was not analyzed. The average time of construction and elaboration stages were 3.2 and 16.2 s, respectively (**Supplementary Table S1**). Both models used a high-pass filter of 0.011 Hz. To confirm that results are not explained by physiological noise, we repeated analyses including the six head motion parameters, outliers (> 0.5 mm mean framewise displacement; Power et al., 2012), and physiological correlates from the aCompCor (Behzadi et al., 2007) variant described in (Pfaffenrot et al., 2025). This variant includes signals from a white-matter ROI (a 4 voxel cube manually placed in adjacent white matter; components chosen to explain 50% variance) and a high residual ROI (> 3 SD of all residuals from the GLM fit; 5 components) putatively sensitive to respiratory and cardiac cycles. The aCompCor regressors were orthogonalized with respect to motion regressors.

For group level assessment, individual hippocampal surfaces were registered to a canonical surface space using HippoMaps (0.1.0, DeKraker et al., 2025) and beta parameters were sampled from volume to each hippocampal surface (*wb_command -volume-to-surface-mapping*) using trilinear interpolation. Topological patterns were characterized for mean activation across hippocampal layers and differences between inner and outer layers (third surface hippocampal side of the boundary surface). For statistical testing, surface overlays were smoothed 5 mm Gaussian smoothing kernel sigma (*wb_command -metric-smoothing*). Statistics used one and two sample t-tests were computed using non-parametric permutation testing using PALM tool (https://github.com/andersonwinkler/PALM; Winkler et al., 2014) and cluster inference on the canonical hippocampal surface.

To assess layer-specificity of VASO and BOLD activation, unsmoothed z-scores were sampled to surfaces and binned and averaged per depth and subfield. Layer-specific VASO and BOLD profiles were compared at group using the Generalized Additive Model (GAM) framework as

implemented by the AFNI PTA tool (Chen et al., 2021) utilizing the mgcv R package (Wood and Scheipl, 2020). This approach treats the cortical depth function as a Multilevel Smoothing Spline (MSS). Specifically, we modeled the smooth effect of layer depth and the interaction between layer and condition as fixed effects, while incorporating inter-subject variability as a random effect. Smoothing parameters were estimated using Restricted Maximum Likelihood (REML). To allow for non-linear complexity in the BOLD profile, the maximum degrees of freedom for the smooth terms were set at $k = 15$. The comparison of the two fMRI contrasts across layers was tested by the Contrast × Layer interaction. Results were FDR-corrected across the other four subfields. We only considered the middle surface of CA4 and dentate gyrus (DG) since the neuronal laminar organization of these subfields is less clear.

Functional connectivity analysis

Connectivity analysis assessed connectivity patterns between areas of the hippocampus and part of the cortex within FOV. Data was preprocessed by regressing out task effects (blocks) and nuisance covariates (aCompCor, six motion parameters, motion outliers of > 0.5 mm FD), and high-pass filtering (0.01 Hz). Data was then sampled to hippocampal inner or outer depths (third surface inside white and pial surfaces). Vertices were then grouped based on subfield and belonging to the anterior or posterior hippocampus (35% and 65% of hippocampal length, respectively; Hackert et al., 2002), and time series defined by vertexwise mean. Background connectivity was then measured as Pearson correlation between seed time-series and brain voxels, and sampled to inner or outer neocortical surfaces. To assess group-level patterns, surfaces were normalized using spherical surface registration (Fischl et al., 1999) and value overlays smoothed 3 mm FWHM on surface to account for individual variability (*mri_surf2surf*). Group-level patterns were assessed using non-parametric permutation testing as for activations.

Functional connectivity based on VASO and BOLD were expected to show similarity in the spatial patterns of task-evoked activation, as they are strongly related to each other and functional boundaries. Further, based on previous literature, we expected relative differences to emerge in the network connectivity of anterior and posterior hippocampus. As the subiculum is a major output region of the hippocampus with neocortical circuits arising primarily from the pyramidal cell layer, we sampled the subiculum middle layer for this network assessment.

Data Availability

The raw neuroimaging data that support the findings of this study is available at OpenNeuro: ds007122.

Competing Interests

Authors declare that they have no competing interests.

Acknowledgments

We thank Dr An Vu for his helpful feedback and discussion.

Funding

Research reported in this publication was supported by the National Institutes of Health (NIH) under award numbers U01-EB025162 (NIBIB), U24-NS129949 (NINDS), and R44-MH129278 (NIMH); and by Weill NeuroHub.

References

Abraham, A., Pedregosa, F., Eickenberg, M., Gervais, P., Mueller, A., Kossaifi, J., Gramfort, A., Thirion, B., Varoquaux, G., 2014. Machine learning for neuroimaging with scikit-learn. Front. Neuroinform. 8, 1–10. https://doi.org/10.3389/fninf.2014.00014

Addis, D.R., Wong, A.T., Schacter, D.L., 2007. Remembering the past and imagining the future: Common and distinct neural substrates during event construction and elaboration. *Neuropsychologia* 45, 1363–1377. https://doi.org/10.1016/j.neuropsychologia.2006.10.016

Ahmadi, K., Stawarczyk, D., Pfaffenrot, V., Gomez, C.A., Kashyap, S., Patai, Z., Norris, D., Axmacher, N., 2024. Laminar profile of hippocampal subfields during spatial navigation. Proc. Intl. Soc. Mag. Reson. Med. 32, 890.

Ahmadi, K., Swegle, S., Kashyap, S., Bouyeure, A., Bandettini, P., Axmacher, N., Huber, L., 2025. Blood volume sensitive laminar fMRI with VASO in human hippocampus: Capabilities and biophysical challenges at clinical 7T scanners. *bioRxiv* [Preprint]. https://doi.org/10.1101/2025.08.25.672075

Aitken, F., Winston, J.S., Muircheartaigh, J.Ó., Carmichael, D., 2025. The potential of laminar fMRI for refining the understanding of epilepsy in humans at the microcircuit level. *OSF Preprints*. https://osf.io/preprints/osf/3e7jv_v1

Amaral, D.G., Witter, M.P., 1989. The Hippocampal Formation, in: Bloom, F.E., Mountcastle, V.B., Geiger, S.R. (Eds.), Handbook of Physiology, Section 1: The Nervous System, Vol. V: Higher Functions of the Brain. American Physiological Society, pp. 311–438.

Angeli, P.A., DiNicola, L.M., Saadon-Grosman, N., Eldaief, M.C., Buckner, R.L., 2025. Specialization of the human hippocampal long axis revisited. Proc. Natl. Acad. Sci. U. S. A. 122, e2422083122. https://doi.org/10.1073/pnas.2422083122

Audrain, S., McAndrews, M.P., 2022. Schemas provide a scaffold for neocortical integration of new memories over time. Nat. Commun. 13, 5795. https://doi.org/10.1038/s41467-022-33517-0

Avants, B., Epstein, C., Grossman, M., Gee, J., 2008. Symmetric diffeomorphic image registration with cross-correlation: Evaluating automated labeling of elderly and neurodegenerative brain. Med. Image Anal. 12, 26–41. https://doi.org/10.1016/j.media.2007.06.004

Beckett, A.J.S., Dadakova, T., Townsend, J., Huber, L., Park, S., Feinberg, D.A., 2020. Comparison of BOLD and CBV using 3D EPI and 3D GRASE for cortical layer functional MRI at 7 T. Magn. Reson. Med. 84, 3128–3145. https://doi.org/10.1002/mrm.28347

Behzadi, Y., Restom, K., Liau, J., Liu, T.T., 2007. A component based noise correction method (CompCor) for BOLD and perfusion based fMRI. *NeuroImage* 37, 90–101. https://doi.org/10.1016/j.neuroimage.2007.04.042

Borne, L., Tian, Y., Lupton, M.K., Van Der Meer, J.N., Jeganathan, J., Paton, B., Koussis, N., Guo, C.C., Robinson, G.A., Fripp, J., Zalesky, A., Breakspear, M., 2023. Functional re-organization of hippocampal-cortical gradients during naturalistic memory processes. *NeuroImage* 271, 119996. https://doi.org/10.1016/j.neuroimage.2023.119996

Braak, H., Del Tredici, K., 2020. From the entorhinal region via the prosubiculum to the dentate fascia: Alzheimer disease-related neurofibrillary changes in the temporal allocortex. J. Neuropathol. Exp. Neurol. 79, 163–175. https://doi.org/10.1093/jnen/nlz123

Brunec, I.K., Bellana, B., Ozubko, J.D., Man, V., Robin, J., Liu, Z.-X., Grady, C., Rosenbaum, R.S., Winocur, G., Barense, M.D., Moscovitch, M., 2018. Multiple scales of representation along the hippocampal anteroposterior axis in humans. Curr. Biol. 28, 2129–2135.e6. https://doi.org/10.1016/j.cub.2018.05.016

Burak, A., Koiso, K., Klein, R., Handwerker, D.A., Huber, L., 2022. Laminar level subcortico-cortical interactions during naturalistic movie viewing. *Organization for Human Brain Mapping (OHBM)*, 2234.

Chen, G., Nash, T.A., Cole, K.M., Kohn, P.D., Wei, S.-M., Gregory, M.D., Eisenberg, D.P., Cox, R.W., Berman, K.F., Shane Kippenhan, J., 2021. Beyond linearity in neuroimaging: Capturing nonlinear relationships with application to longitudinal studies. *NeuroImage* 233, 117891. https://doi.org/10.1016/j.neuroimage.2021.117891

Clark, J.M., Paivio, A., 2004. Extensions of the Paivio, Yuille, and Madigan (1968) norms. Behav. Res. Methods Instrum. Comput. 36, 371–383. https://doi.org/10.3758/BF03195584

Dale, A.M., Fischl, B., Sereno, M.I., 1999. Cortical surface-based analysis: I. segmentation and surface reconstruction. *NeuroImage* 9, 179–194. https://doi.org/10.1006/nimg.1998.0395

Dalton, M.A., McCormick, C., Maguire, E.A., 2019. Differences in functional connectivity along the anterior-posterior axis of human hippocampal subfields. *NeuroImage* 192, 38–51. https://doi.org/10.1016/j.neuroimage.2019.02.066

De Flores, R., Das, S.R., Xie, L., Wisse, L.E.M., Lyu, X., Shah, P., Yushkevich, P.A., Wolk, D.A., 2022. Medial temporal lobe networks in Alzheimer's disease: Structural and molecular vulnerabilities. J. Neurosci. 42, 2131–2141. https://doi.org/10.1523/jneurosci.0949-21.2021

Dehaene, S., Molko, N., Cohen, L., Wilson, A.J., 2004. Arithmetic and the brain. Curr. Opin. Neurobiol. 14, 218–224. https://doi.org/10.1016/j.conb.2004.03.008

DeKraker, J., Cabalo, D.G., Royer, J., Ngo, A., Khan, A.R., Karat, B.G., Benkarim, O., Rodriguez-Cruces, R., Frauscher, B., Pana, R., Hansen, J.Y., Misic, B., Valk, S.L., Lau, J.C., Kirschner, M., Bernasconi, A., Bernasconi, N., Muenzing, S.E.A., Axer, M., Amunts, K., Evans, A.C., Bernhardt, B.C., 2025. HippoMaps: multiscale cartography of human hippocampal organization. Nat. Methods 22, 2211–2222. https://doi.org/10.1038/s41592-025-02783-3

DeKraker, J., Haast, R.A., Yousif, M.D., Karat, B., Lau, J.C., Köhler, S., Khan, A.R., 2022. Automated hippocampal unfolding for morphometry and subfield segmentation with HippUnfold. *eLife* 11, e77945. https://doi.org/10.7554/eLife.77945

DiNicola, L.M., Braga, R.M., Buckner, R.L., 2020. Parallel distributed networks dissociate episodic and social functions within the individual. J. Neurophysiol. 123, 1144–1179. https://doi.org/10.1152/jn.00529.2019

Dresbach, S., Huber, L., Gulban, O.F., Goebel, R., 2023. Layer-fMRI VASO with short stimuli and event-related designs at 7 T. *NeuroImage* 279, 120293. https://doi.org/10.1016/j.neuroimage.2023.120293

Duvernoy, H.M., Cattin, F., Risold, P.-Y., 2005. The human hippocampus: functional anatomy, vascularization and serial sections with MRI. Springer.

Duvernoy, H.M., Delon, S., Vannson, J.L., 1981. Cortical blood vessels of the human brain. Brain Res. Bull. 7, 519–579. https://doi.org/10.1016/0361-9230(81)90007-1

Faes, L.K., De Martino, F., Huber, L., 2023. Cerebral blood volume sensitive layer-fMRI in the human auditory cortex at 7T: Challenges and capabilities. *PLoS ONE* 18, e0280855. https://doi.org/10.1371/journal.pone.0280855

Faes, L.K., Lage-Castellanos, A., Valente, G., Yu, Z., Cloos, M.A., Vizioli, L., Moeller, S., Yacoub, E., De Martino, F., 2024. Evaluating the effect of denoising submillimeter auditory fMRI data with NORDIC. *Imaging Neurosci.* 2, 1–18. https://doi.org/10.1162/imag_a_00270

Feinberg, D.A., Beckett, A.J.S., Vu, A.T., Stockmann, J., Huber, L., Ma, S., Ahn, S., Setsompop, K., Cao, X., Park, S., Liu, C., Wald, L.L., Polimeni, J.R., Mareyam, A., Gruber, B., Stirnberg, R., Liao, C., Yacoub, E., Davids, M., Bell, P., Rummert, E., Koehler, M., Potthast, A., Gonzalez-Insua, I., Stocker, S., Gunamony, S., Dietz, P., 2023. Next-generation MRI scanner designed for ultra-high-resolution human brain imaging at 7 Tesla. Nat. Methods 20, 2048–2057. https://doi.org/10.1038/s41592-023-02068-7

Feinberg, D.A., Harel, N., Ramanna, S., Ugurbil, K., Yacoub, E., 2008. Sub-millimeter single-shot 3D GRASE with inner volume selection for T2-weighted fMRI applications at 7 Tesla. *Proc. Intl. Soc. Mag. Reson. Med.* 16, 2373.

Felleman, D.J., Van Essen, D.C., 1991. Distributed hierarchical processing in the primate cerebral cortex. Cereb. Cortex 1, 1–47. https://doi.org/10.1093/cercor/1.1.1-a

Fischl, B., Sereno, M.I., Tootell, R.B.H., Dale, A.M., 1999. High-resolution intersubject averaging and a coordinate system for the cortical surface. Hum. Brain Mapp. 8, 272–284. https://doi.org/10.1002/(SICI)1097-0193(1999)8:4<272::AID-HBM10>3.0.CO;2-4

Franzmeier, N., Neitzel, J., Rubinski, A., Smith, R., Strandberg, O., Ossenkoppele, R., Hansson, O., Ewers, M., Alzheimer's Disease Neuroimaging Initiative (ADNI), 2020. Functional brain architecture is associated with the rate of tau accumulation in Alzheimer's disease. Nat. Commun. 11, 347. https://doi.org/10.1038/s41467-019-14159-1

Gilmore, A.W., Quach, A., Kalinowski, S.E., Gotts, S.J., Schacter, D.L., Martin, A., 2021. Dynamic content reactivation supports naturalistic autobiographical recall in humans. J. Neurosci. 41, 153–166. https://doi.org/10.1523/JNEUROSCI.1490-20.2020

Gómez-Isla, T., Price, J.L., McKeel Jr., D.W., Morris, J.C., Growdon, J.H., Hyman, B.T., 1996. Profound loss of layer II entorhinal cortex neurons occurs in very mild Alzheimer's disease. J. Neurosci. 16, 4491–4500. https://doi.org/10.1523/JNEUROSCI.16-14-04491.1996

Gorgolewski, K., Burns, C.D., Madison, C., Clark, D., Halchenko, Y.O., Waskom, M.L., Ghosh, S.S., 2011. Nipype: a flexible, lightweight and extensible neuroimaging data processing framework in Python. Front. Neuroinform. 5, 13. https://doi.org/10.3389/fninf.2011.00013

Greve, D.N., Fischl, B., 2009. Accurate and robust brain image alignment using boundary-based registration. *NeuroImage* 48, 63–72. https://doi.org/10.1016/j.neuroimage.2009.06.060

Grieco, S.F., Holmes, T.C., Xu, X., 2023. Probing neural circuit mechanisms in Alzheimer's disease using novel technologies. Mol. Psychiatry 28, 4407–4420. https://doi.org/10.1038/s41380-023-02018-x

Haarsma, J., Kok, P., 2025. How layer-specific fMRI can contribute to understanding perceptual disturbances across psychiatric disorders. Curr. Top. Behav. Neurosci. 74, 41–72. https://doi.org/10.1007/7854_2025_595

Haast, R.A.M., Kashyap, S., Ivanov, D., Yousif, M.D., DeKraker, J., Poser, B.A., Khan, A.R., 2024. Insights into hippocampal perfusion using high-resolution, multi-modal 7T MRI. Proc. Natl. Acad. Sci. U. S. A. 121, e2310044121. https://doi.org/10.1073/pnas.2310044121

Hackert, V.H., Den Heijer, T., Oudkerk, M., Koudstaal, P.J., Hofman, A., Breteler, M.M.B., 2002. Hippocampal head size associated with verbal memory performance in nondemented elderly. *NeuroImage* 17, 1365–1372. https://doi.org/10.1006/nimg.2002.1248

Harrison, P.J., 2004. The hippocampus in schizophrenia: a review of the neuropathological evidence and its pathophysiological implications. *Psychopharmacology* 174, 151–162. https://doi.org/10.1007/s00213-003-1761-y

Hofstetter, C., Achaibou, A., Vuilleumier, P., 2012. Reactivation of visual cortex during memory retrieval: Content specificity and emotional modulation. *NeuroImage* 60, 1734–1745. https://doi.org/10.1016/j.neuroimage.2012.01.110

Huber, L., Goense, J., Kennerley, A.J., Trampel, R., Guidi, M., Reimer, E., Ivanov, D., Neef, N., Gauthier, C.J., Turner, R., Möller, H.E., 2015. Cortical lamina-dependent blood volume changes in human brain at 7 T. *NeuroImage* 107, 23–33. https://doi.org/10.1016/j.neuroimage.2014.11.046

Huber, L., Ivanov, D., Krieger, S.N., Streicher, M.N., Mildner, T., Poser, B.A., Möller, H.E., Turner, R., 2014. Slab-selective, BOLD-corrected VASO at 7 Tesla provides measures of cerebral blood volume reactivity with high signal-to-noise ratio. Magn. Reson. Med. 72, 137–148. https://doi.org/10.1002/mrm.24916

Huber, L., Poser, B.A., Kaas, A.L., Fear, E.J., Dresbach, S., Berwick, J., Goebel, R., Turner, R., Kennerley, A.J., 2021. Validating layer-specific VASO across species. *NeuroImage* 237, 118195. https://doi.org/10.1016/j.neuroimage.2021.118195

Kay, K., 2022. The risk of bias in denoising methods: Examples from neuroimaging. *PLoS ONE* 17, e0270895. https://doi.org/10.1371/journal.pone.0270895

Kerchner, G.A., Deutsch, G.K., Zeineh, M., Dougherty, R.F., Saranathan, M., Rutt, B.K., 2012. Hippocampal CA1 apical neuropil atrophy and memory performance in Alzheimer's disease. *NeuroImage* 63, 194–202. https://doi.org/10.1016/j.neuroimage.2012.06.048

Knudsen, L., Vizioli, L., De Martino, F., Faes, L.K., Handwerker, D.A., Moeller, S., Bandettini, P.A., Huber, L., 2025. NORDIC denoising on VASO data. Front. Neurosci. 18, 1499762. https://doi.org/10.3389/fnins.2024.1499762

Koster, R., Chadwick, M.J., Chen, Y., Berron, D., Banino, A., Düzel, E., Hassabis, D., Kumaran, D., 2018. Big-loop recurrence within the hippocampal system supports integration of information across episodes. *Neuron* 99, 1342–1354.e6. https://doi.org/10.1016/j.neuron.2018.08.009

Kwon, Y.H., Salvo, J.J., Anderson, N.L., Edmonds, D., Holubecki, A.M., Lakshman, M., Yoo, K., Yeo, B.T.T., Kay, K., Gratton, C., Braga, R.M., 2025. Situating the salience and parietal memory networks in the context of multiple parallel distributed networks using precision functional mapping. *Cell Rep.* 44, 115207. https://doi.org/10.1016/j.celrep.2024.115207

Lace, G., Savva, G.M., Forster, G., De Silva, R., Brayne, C., Matthews, F.E., Barclay, J.J., Dakin, L., Ince, P.G., Wharton, S.B., 2009. Hippocampal tau pathology is related to neuroanatomical connections: an ageing population-based study. *Brain* 132, 1324–1334. https://doi.org/10.1093/brain/awp059

Leal, S.L., Yassa, M.A., 2018. Integrating new findings and examining clinical applications of pattern separation. Nat. Neurosci. 21, 163–173. https://doi.org/10.1038/s41593-017-0065-1

Leelaarporn, P., Dalton, M.A., Stirnberg, R., Stöcker, T., Spottke, A., Schneider, A., McCormick, C., 2024. Hippocampal subfields and their neocortical interactions during autobiographical memory. *Imaging Neurosci.* 2, 1–13. https://doi.org/10.1162/imag_a_00105

Lu, H., Golay, X., Pekar, J.J., Van Zijl, P.C.M., 2003. Functional magnetic resonance imaging based on changes in vascular space occupancy. Magn. Reson. Med. 50, 263–274. https://doi.org/10.1002/mrm.10519

Maass, A., Schütze, H., Speck, O., Yonelinas, A., Tempelmann, C., Heinze, H.-J., Berron, D., Cardenas-Blanco, A., Brodersen, K.H., Enno Stephan, K., Düzel, E., 2014. Laminar activity in the hippocampus and entorhinal cortex related to novelty and episodic encoding. Nat. Commun. 5, 5547. https://doi.org/10.1038/ncomms6547

Marcus, D.S., Harwell, J., Olsen, T., Hodge, M., Glasser, M.F., Prior, F., Jenkinson, M., Laumann, T., Curtiss, S.W., Van Essen, D.C., 2011. Informatics and data mining tools and strategies for the Human Connectome Project. Front. Neuroinform. 5, 4. https://doi.org/10.3389/fninf.2011.00004

Mather, M., Harley, C.W., 2016. The locus coeruleus: Essential for maintaining cognitive function and the aging brain. Trends Cogn. Sci. 20, 214–226. https://doi.org/10.1016/j.tics.2016.01.001

McCormick, C., St-Laurent, M., Ty, A., Valiante, T.A., McAndrews, M.P., 2015. Functional and effective hippocampal–neocortical connectivity during construction and elaboration of autobiographical memory retrieval. Cereb. Cortex 25, 1297–1305. https://doi.org/10.1093/cercor/bht324

Moeller, S., Pisharady, P.K., Ramanna, S., Lenglet, C., Wu, X., Dowdle, L., Yacoub, E., Uğurbil, K., Akçakaya, M., 2021. NOise reduction with DIstribution Corrected (NORDIC) PCA in dMRI with complex-valued parameter-free locally low-rank processing. *NeuroImage* 226, 117539. https://doi.org/10.1016/j.neuroimage.2020.117539

Olesen, J.L., Ianus, A., Østergaard, L., Shemesh, N., Jespersen, S.N., 2023. Tensor denoising of multidimensional MRI data. Magn. Reson. Med. 89, 1160–1172. https://doi.org/10.1002/mrm.29478

Olman, C.A., Inati, S., Heeger, D.J., 2007. The effect of large veins on spatial localization with GE BOLD at 3 T: Displacement, not blurring. *NeuroImage* 34, 1126–1135. https://doi.org/10.1016/j.neuroimage.2006.08.045

Oshio, K., Feinberg, D.A., 1991. GRASE (Gradient-and Spin-Echo) imaging: A novel fast MRI technique. Magn. Reson. Med. 20, 344–349. https://doi.org/10.1002/mrm.1910200219

Pfaffenrot, V., Bouyeure, A., Gomes, C.A., Kashyap, S., Axmacher, N., Norris, D.G., 2025. Characterizing BOLD activation patterns in the human hippocampus with laminar fMRI. *Imaging Neurosci.* 3, imag_a_00532. https://doi.org/10.1162/imag_a_00532

Poppenk, J., Evensmoen, H.R., Moscovitch, M., Nadel, L., 2013. Long-axis specialization of the human hippocampus. Trends Cogn. Sci. 17, 230–240. https://doi.org/10.1016/j.tics.2013.03.005

Power, J.D., Barnes, K.A., Snyder, A.Z., Schlaggar, B.L., Petersen, S.E., 2012. Spurious but systematic correlations in functional connectivity MRI networks arise from subject motion. *NeuroImage* 59, 2142–2154. https://doi.org/10.1016/j.neuroimage.2011.10.018

Rane, S., Talati, P., Donahue, M.J., Heckers, S., 2016. Inflow-vascular space occupancy (iVASO) reproducibility in the hippocampus and cortex at different blood water nulling times. Magn. Reson. Med. 75, 2379–2387. https://doi.org/10.1002/mrm.25836

Rolls, E.T., 2013. The mechanisms for pattern completion and pattern separation in the hippocampus. Front. Syst. Neurosci. 7, 74. https://doi.org/10.3389/fnsys.2013.00074

Rutland, J.W., Brown, S., Verma, G., Feldman, R.E., Sharma, H., Markowitz, M., Schneider, M., Delman, B.N., Murrough, J., Balchandani, P., 2019. Hippocampal subfield-specific connectivity findings in major depressive disorder: A 7 Tesla diffusion MRI study. J. Psychiatr. Res. 111, 186–192. https://doi.org/10.1016/j.jpsychires.2019.02.008

Tang, L., Pruitt, P.J., Yu, Q., Homayouni, R., Daugherty, A.M., Damoiseaux, J.S., Ofen, N., 2020. Differential functional connectivity in anterior and posterior hippocampus supporting the development of memory formation. Front. Hum. Neurosci. 14, 204. https://doi.org/10.3389/fnhum.2020.00204

Vizioli, L., Moeller, S., Dowdle, L., Akçakaya, M., De Martino, F., Yacoub, E., Uğurbil, K., 2021. Lowering the thermal noise barrier in functional brain mapping with magnetic resonance imaging. Nat. Commun. 12, 5181. https://doi.org/10.1038/s41467-021-25431-8

Vos De Wael, R., Larivière, S., Caldairou, B., Hong, S.-J., Margulies, D.S., Jefferies, E., Bernasconi, A., Smallwood, J., Bernasconi, N., Bernhardt, B.C., 2018. Anatomical and microstructural determinants of hippocampal subfield functional connectome embedding. Proc. Natl. Acad. Sci. U. S. A. 115, 10154–10159. https://doi.org/10.1073/pnas.1803667115

Warrington, O., Graedel, N.N., Callaghan, M.F., Kok, P., 2025. Communication of perceptual predictions from the hippocampus to the deep layers of the parahippocampal cortex. Sci. Adv. 11, eads4970. https://doi.org/10.1126/sciadv.ads4970

Winkler, A.M., Ridgway, G.R., Webster, M.A., Smith, S.M., Nichols, T.E., 2014. Permutation inference for the general linear model. *NeuroImage* 92, 381–397. https://doi.org/10.1016/j.neuroimage.2014.01.060

Wood, S.N., Scheipl, F., 2020. gamm4: Generalized additive mixed models using ’mgcv’ and ’lme4’. *R package version 0.2-6*. https://CRAN.R-project.org/package=gamm4.

Zaretskaya, N., Fischl, B., Reuter, M., Renvall, V., Polimeni, J.R., 2018. Advantages of cortical surface reconstruction using submillimeter 7 T MEMPRAGE. *NeuroImage* 165, 11–26. https://doi.org/10.1016/j.neuroimage.2017.09.060

Zhang, K., Chen, L., Li, Y., Paez, A.G., Miao, X., Cao, D., Gu, C., Pekar, J.J., Van Zijl, P.C.M., Hua, J., Bakker, A., 2023. Differential laminar activation dissociates encoding and retrieval in the human medial and lateral entorhinal cortex. J. Neurosci. 43, 2874–2884. https://doi.org/10.1523/jneurosci.1488-22.2023

Zheng, A., Montez, D.F., Marek, S., Gilmore, A.W., Newbold, D.J., Laumann, T.O., Kay, B.P., Seider, N.A., Van, A.N., Hampton, J.M., Alexopoulos, D., Schlaggar, B.L., Sylvester, C.M., Greene, D.J., Shimony, J.S., Nelson, S.M., Wig, G.S., Gratton, C., McDermott, K.B., Raichle, M.E., Gordon, E.M., Dosenbach, N.U.F., 2021. Parallel hippocampal-parietal circuits for self- and goal-oriented processing. Proc. Natl. Acad. Sci. U. S. A. 118, e2101743118. https://doi.org/10.1073/pnas.2101743118